Improved Modelling of Solidification in Stainless Steels

The model used in JMatPro® to describe the solidification behaviour of stainless steels considers the microstructure as "frozen" at the solidus. The validity of this assumption very much depends on the type of stainless steel. While it is reasonable for (stable) austenitic and ferritic stainless steels, it fails to capture other types of microstructures. This report describes an extended model, introduced in JMatPro® v11, which considers further potential phase transformations thereby leading to improved predictions.

Performance of Conventional Methods

Modelling of solidification in stainless steels requires taking into account, at least to some extent, the effect of fast diffusion of certain solute elements in the solid phase. Conventional methods[1–3] include the equilibrium lever rule which assumes infinitely fast diffusion for all substitutional and interstitial components, and the modified Scheil-Gulliver model which restricts this effect to interstitials (namely, C and N). Prior to version 11, the solidification module for stainless steels in JMatPro® was based on the modified Scheil-Gulliver model, but it is instructive to compare the two approaches. Figures 1–5 show the microstructural evolutions predicted by these models for a number of stainless steels whose compositions

Table 1: *Chemical compositions of the stainless steel alloys considered in this study (in wt%).*

	Fe	C	Cr	Cu	Mn	Mo	N	Ni	Si
904L	bal.	0.02	21.0	1.5	–	4.5	0.073	25.0	–
304L	bal.	0.022	18.1	–	1.81	–	–	9.2	0.41
SAF2507	bal.	0.01	25.0	–	1.0	3.8	0.28	7.0	0.4
420	bal.	0.2	13.0	–	0.5	–	–	0.5	0.5
430F	bal.	0.12	17.0	–	1.25	0.6	–	–	1.0

are listed in Table 1. These compositions are chosen as typical examples of five possible types of stainless steels, characterised by their high-temperature and ultimate room-temperature microstructures:

- *Austenitic (stable)* [904L] – Alloys of this type are austenitic at room temperature and austenite is also the primary phase during solidification. As illustrated in Fig. 1, both equilibrium and modified Scheil-Gulliver models capture this behaviour correctly, although a residual amount of ferrite may

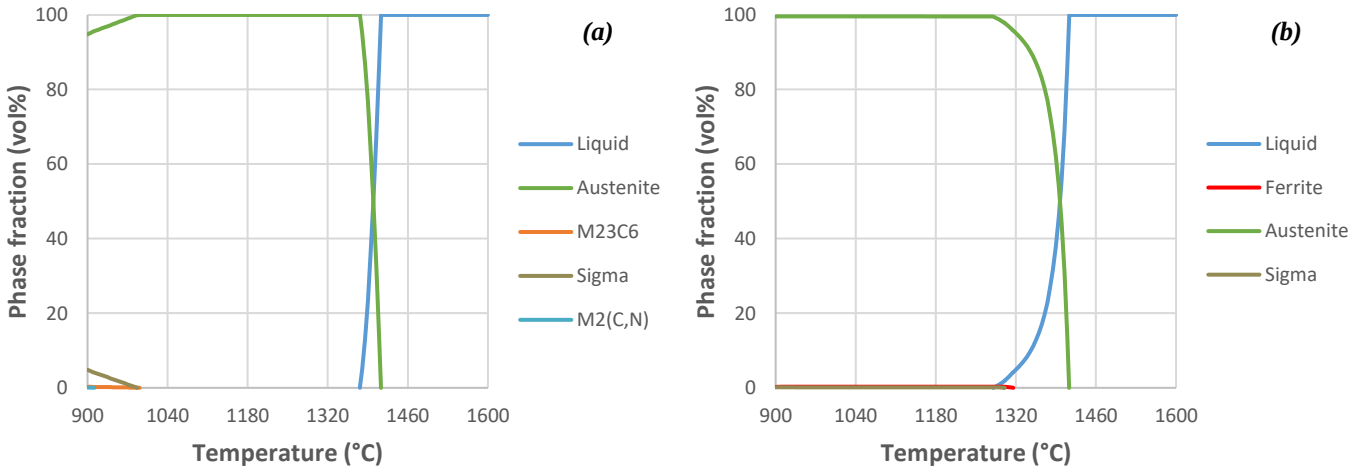

Figure 1: *Phase fraction vs temperature curves obtained using equilibrium (a) and modified Scheil-Gulliver (b) models for stainless steel 904L.*

be predicted using the latter. The main difference between the models is in the predicted freezing ranges, with the modified Scheil-Gulliver model giving superior results.[1]

- *Austenitic (peritectic)* [304L] – Alloys of this type are also austenitic at room temperature, but the primary phase during solidification is ferrite. Austenite is usually created upon decreasing the temperature via a peritectic transformation.[4] As depicted in Fig. 2, the equilibrium approach can be used to model the growth of austenite at the expense of liquid and ferrite, but this is not possible in the framework of the modified Scheil-Gulliver model, which freezes the microstructure and overestimates the amount of ferrite ultimately obtained.

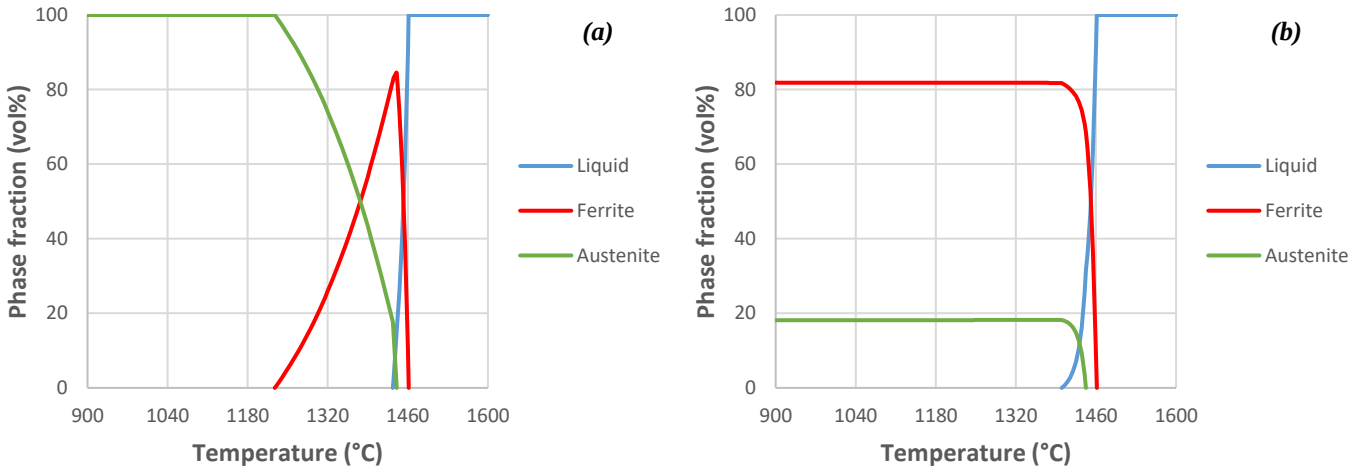

Figure 2: *Phase fraction vs temperature curves obtained using equilibrium (a) and modified Scheil-Gulliver (b) models for stainless steel 304L.*

- *Duplex* [SAF2507] – In this case, the room-temperature microstructure consists of about 50% austenite and 50% ferrite after heat treatment at the duplex temperature. The equilibrium model can reproduce this microstructure at elevated temperatures, but in order to preserve it as the temperature decreases it may be necessary to suppress formation of certain secondary phases [see Fig. 3(a)]. As shown in Fig. 3(b), this is accounted for in the modified Scheil-Gulliver model but, similarly to the peritectic case, it generally leads to an excessive amount of ferrite.

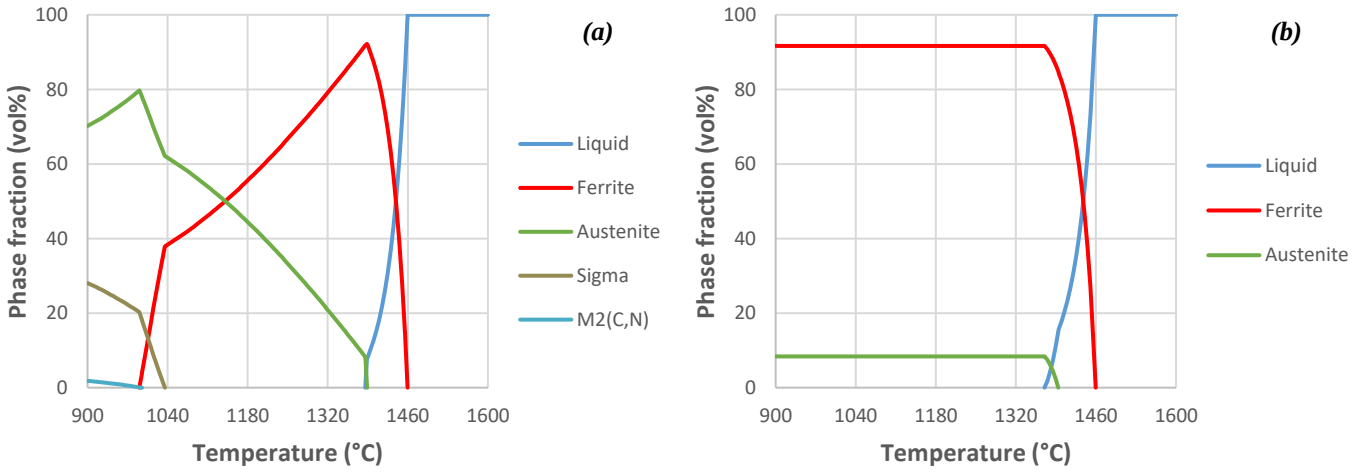

Figure 3: *Phase fraction vs temperature curves obtained using equilibrium (a) and modified Scheil-Gulliver (b) models for stainless steel SAF2507.*

- *Martensitic* [420] – Alloys of this type are martensitic at room temperature. Solidification proceeds by first forming ferrite and then austenite via a peritectic transformation. Martensite is produced at lower temperatures from the solid-state decomposition of austenite.[5,6] Both equilibrium and

modified Scheil-Gulliver models lack key ingredients to describe this behaviour in full, as seen in Fig. 4.

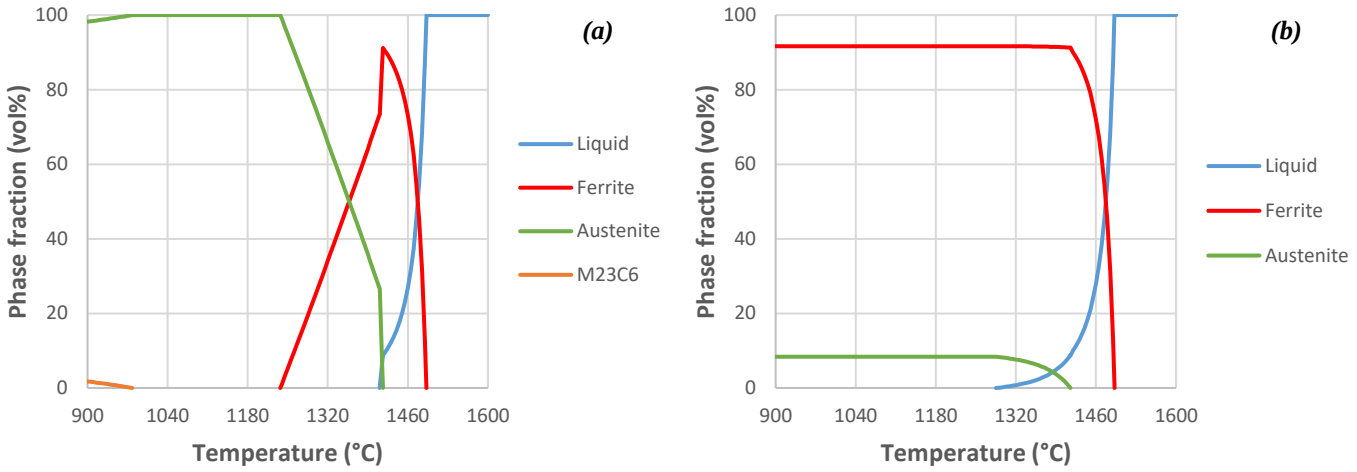

Figure 4: *Phase fraction vs temperature curves obtained using equilibrium (a) and modified Scheil-Gulliver (b) models for stainless steel 420.*

- *Ferritic* [430F] – Alloys of this type are ferritic at room temperature and ferrite is also the primary phase during solidification. As shown in Fig. 5, the microstructural evolution at elevated temperatures is captured correctly by both equilibrium and modified Scheil-Gulliver models, with very similar results obtained for the freezing ranges. The equilibrium approach may predict considerable formation of austenite below the solidus, but it usually disappears at around 900 °C. This is ignored in the modified Scheil-Gulliver model which generally leads to a negligible amount of austenite. In this case, neglecting solid-state transformations is a more convenient description.

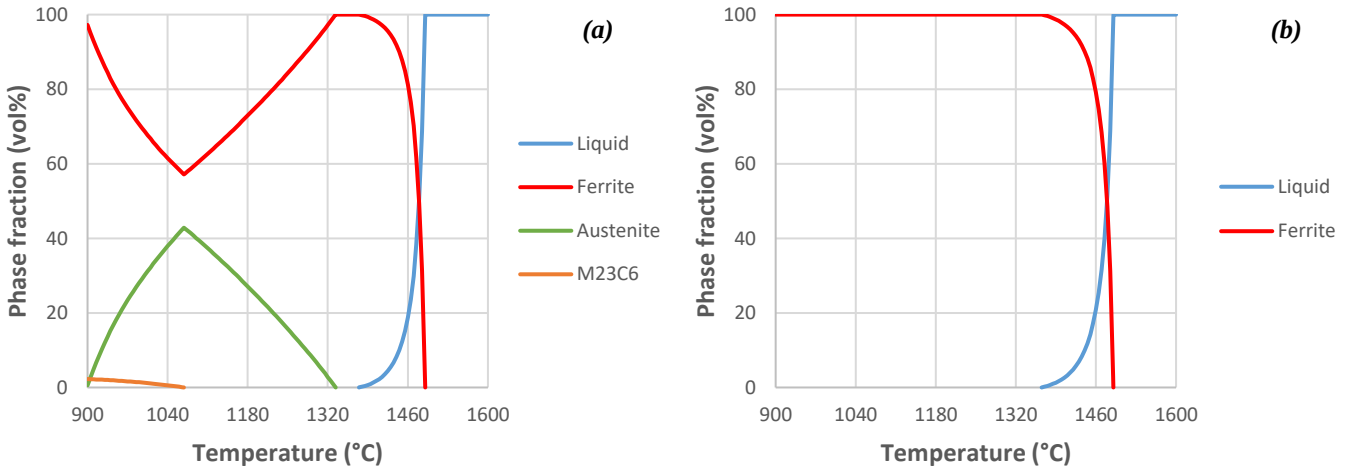

Figure 5: *Phase fraction vs temperature curves obtained using equilibrium (a) and modified Scheil-Gulliver (b) models for stainless steel 430F.*

Improved Procedure for Peritectic, Duplex, and Martensitic Stainless Steels

It is immediately apparent that the modified Scheil-Gulliver model is appropriate to describe the solidification behaviour of stable austenitic and ferritic stainless steels, but further transformations need to be considered for the prediction of peritectic austenitic, duplex, and martensitic microstructures. In particular, these types of stainless steels require modelling the peritectic growth of austenite during solidification, and subsequent ferrite-to-austenite transformation, as well as the kinetics of austenite decomposition at lower temperatures.

In principle, modelling the growth of austenite at the expense of liquid and ferrite requires the numerical solution of a diffusion problem with multiple moving boundaries. This is especially complex due to the multicomponent nature of commercial alloys and the need to consider a two-dimensional system as, in general, austenite and ferrite can both exist in equilibrium with the liquid over a wide range of temperatures. Instead, a simplified strategy, conceptually similar to early work by Fredriksson,[4] is adopted here.

First, a base calculation is performed using the modified Scheil-Gulliver (SG) model. Then, at each temperature step below the peritectic point at which austenite starts to form, two calculation routes are established, considering only the liquid (L), ferrite (δ), and austenite (γ) phases:

1. The average composition of the two-phase field $L_{SG} + \delta_{SG}$ is determined and used to calculate a new three-phase equilibrium, $L_1 + \delta_1 + \gamma_1$. The obtained liquid and ferrite replace the results from the base calculation, while the new austenite is added to the pre-existing one. All phase fractions are adjusted accordingly.
2. Similarly to the above, a three-phase equilibrium $L_2 + \delta_2 + \gamma_2$ is sought, but the average composition of the three-phase field $L_{SG} + \delta_{SG} + \gamma_{SG}$ is used instead. All resulting phases replace those from the base calculation, with the phase fractions updated accordingly.

In both cases, once the liquid is no longer present a new solidus emerges and the final two- or three-phase field average composition is used to continue the procedure in the solid state, following the same rules but considering only ferrite and austenite. The first calculation route essentially amounts to modelling the peritectic solidification sequence $L + \delta \rightarrow L + \delta + \gamma$, and the subsequent $\delta \rightarrow \gamma$ transformation, using stepwise equilibrium calculations, while the second route should be very close to equilibrium solidification with the nominal alloy composition.

The final solidification path is determined by following the route that yields the lowest amount of ferrite. Initially, this will almost always be route 1, but a crossover to route 2 is expected to occur as the temperature decreases. In this way, the proposed method will smoothly move from the modified Scheil-Gulliver result to the equilibrium lever rule case.

The procedure is completed by further taking into account the solid-state decomposition of austenite into martensite (and potentially α-ferrite, pearlite, and bainite). This is achieved following the same model used in the JMatPro® quench properties calculation for general steels, which has been described in detail elsewhere.[5,6] By default, it is assumed that the decomposition starts immediately after δ-ferrite is fully transformed into austenite, or at 900 °C if the transformation is not complete at higher temperatures. It is also possible to start from a user-defined "austenitisation" temperature, which allows for some retained ferrite to be present at room temperature.

Figures 6–8 show the microstructural evolutions calculated with the extended model for alloys 304L, SAF2507, and 420, considering a cooling rate of 1 °C/s and a grain size of 500 μm in the kinetics of

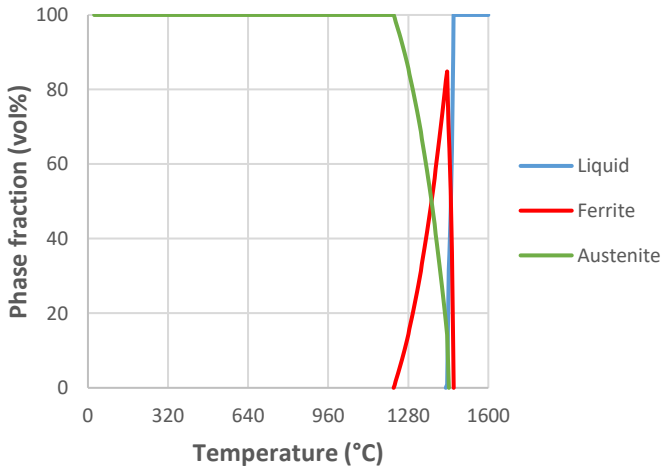

Figure 6: *Phase fraction vs temperature curves obtained using the extended model introduced in JMatPro® v11 for stainless steel 304L.*

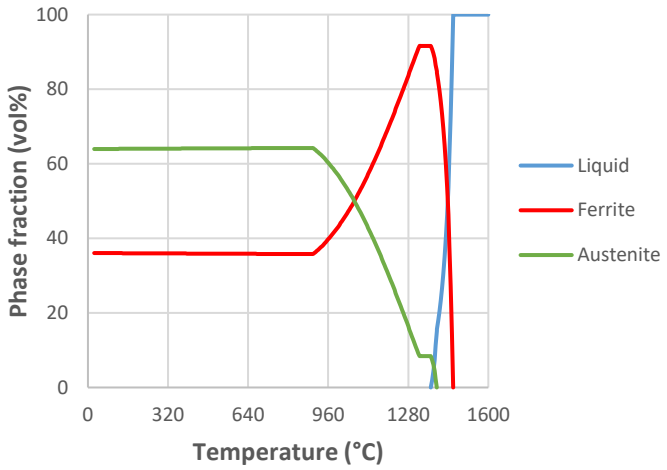

Figure 7: *Phase fraction vs temperature curves obtained using the extended model introduced in JMatPro® v11 for stainless steel SAF2507.*

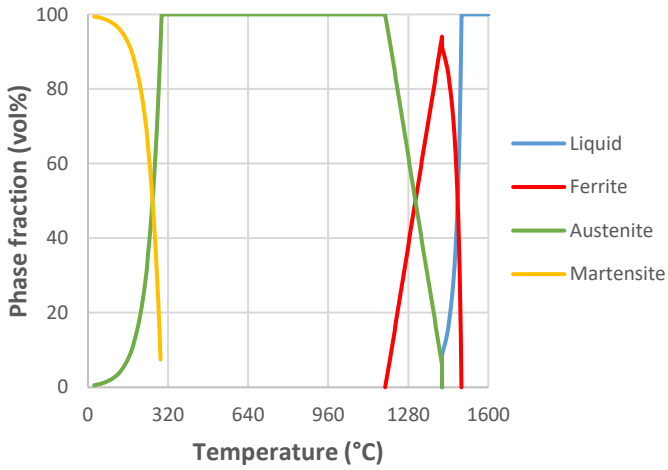

Figure 8: *Phase fraction vs temperature curves obtained using the extended model introduced in JMatPro® v11 for stainless steel 420.*

austenite decomposition. As can be seen by comparing Figs. 6 and 2(a), the temperature dependence obtained for stainless steel 304L closely matches the equilibrium model result, with ferrite completely consumed in the peritectic transformation. The austenite formed is too stable and no further phase transformations are observed, leading to the expected austenitic microstructure. Comparison between Figs. 7 and 3 reveals that for SAF2507 a mixed result is obtained, with the evolution in the mushy zone matching the modified Scheil-Gulliver model, and the subsequent ferrite-to-austenite transformation in the solid state resembling the equilibrium approach but with formation of secondary phases suspended. The austenite is too stable in this case as well, and no decomposition products are seen. A mixture of about 60% austenite and 40% ferrite is obtained at room temperature, not far from an ideal duplex microstructure. For stainless steel 420 the high-temperature evolution is very similar to the equilibrium model prediction [see Figs. 8 and 4(a)]. In contrast to the peritectic and duplex alloys, in this case the austenite starts to transform into martensite at around 300 °C and a fully martensitic microstructure is obtained at room temperature, as expected for conventional cooling rates.

It should be noted that the changes in microstructural evolution are also reflected in the predictions of physical and thermophysical properties. This is illustrated in Fig. 9 for the temperature-dependent thermal conductivity and Young's modulus of stainless steel 304L. Results obtained using the modified Scheil-Gulliver approach and the extended model described here are compared against experimental data.[7,8] The different predictions for the amounts and compositions of ferrite and austenite lead to differences in the calculated property curves, especially in the solid state, with the new model giving a much closer match with experiments. Similar improvements are also expected for duplex and martensitic stainless steels.

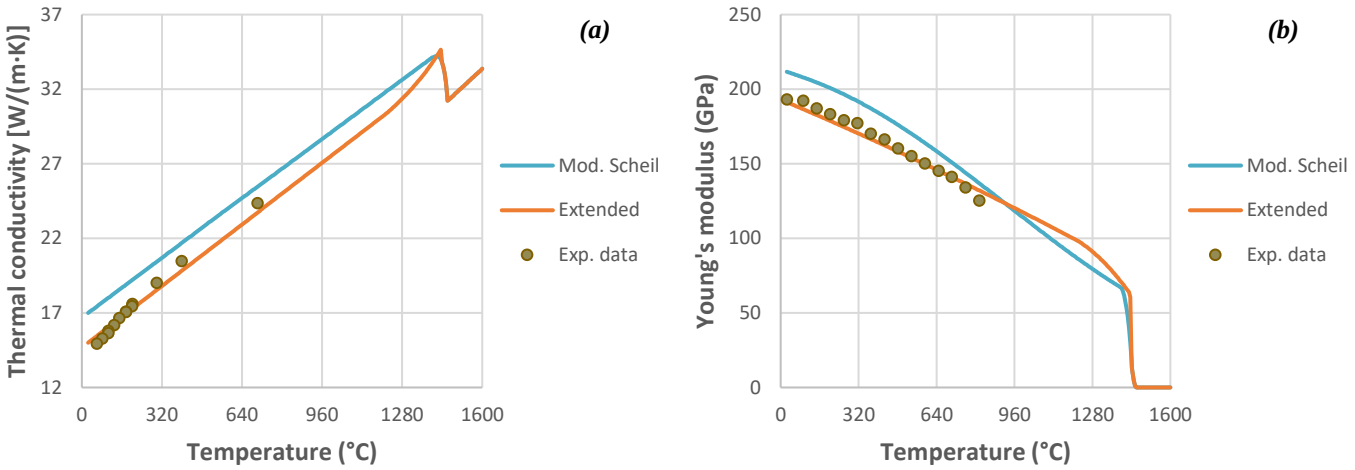

Figure 9: *Thermal conductivity (a) and Young's modulus (b) vs temperature for stainless steel 304L. The modified Scheil-Gulliver and extended model predictions are compared against experimental data from Refs. 7 and 8.*

Summary

A new procedure, introduced in JMatPro® v11, has been described for modelling solidification in stainless steels. It extends the modified Scheil-Gulliver model of previous versions by taking into account the peritectic growth of austenite during solidification, and subsequent ferrite-to-austenite transformation and austenite decomposition in the solid state. The addition of such phase transformations leads to an increased predictive capability of the model, which is suitable for stable and peritectic austenitic, duplex, martensitic, and ferritic stainless steels. Improved descriptions of the microstructural evolution as well as accurate predictions of physical and thermophysical properties during solidification have been demonstrated.

References

1. N. Saunders, "Applicability of the equilibrium and 'Scheil model' to solidification in multi-component alloys", in *Solidification Processing 1997*, edited by J. Beech and H. Jones (University of Sheffield, 1997), p. 362
2. N. Saunders, X. Li, A. P. Miodownik, and J.-Ph. Schillé, "Modelling of the thermo-physical and physical properties relevant to solidification", in *Modelling of Casting, Welding and Advanced Solidification Processes X*, edited by D. Stefanescu, J. A. Warren, M. R. Jolly, and M. J. M. Krane (TMS, Warrendale, PA, 2003), p. 669
3. N. Saunders, Z. Guo, A. P. Miodownik, and J.-Ph. Schillé, "Thermo-physical and physical properties for use in solidification modelling of multi-component alloys", in *Solidification and Crystallization*, edited by D. M. Herlach (Wiley, 2004), p. 82
4. H. Fredriksson, "The mechanism of the peritectic reaction in iron-base alloys", *Metal Science* **10**, 77 (1976)
5. N. Saunders, Z. Guo, X. Li, A. P. Miodownik, and J.-Ph. Schillé, "The calculation of TTT and CCT diagrams for general steels", Internal report, Sente Software Ltd (2004)
6. Z. Guo, N. Saunders, A. P. Miodownik, and J.-Ph. Schillé, "Modelling phase transformations and material properties critical to the prediction of distortion during the heat treatment of steels", *International Journal of Microstructure and Materials Properties* **4**, 187 (2009)
7. R. S. Graves, T. G. Kollie, D. L. McElroy, and K. E. Gilchrist, "The thermal conductivity of AISI 304L stainless steel", *International Journal of Thermophysics* **12**, 409 (1991)
8. Nickel Development Institute, "High-temperature characteristics of stainless steels", *A Designers' Handbook Series*, No. 9004